Monocular Accommodation Response to Random Defocus Changes Induced by a Tuneable Lens

Najnin Sharmin* and Brian Vohnsen

Advanced Optical Imaging Group, School of Physics, University College Dublin, Dublin 4, Ireland

*Email: najnin.sharmin@ucdconnect.ie

Keywords: accommodation, defocus, eye model, retina model, geometrical optics

Accommodation of the human eye relies on multiple factors and visual cues that include object size, monochromatic and chromatic aberrations, and vergence. Yet, even in monocular conditions, accommodation corrects for defocus. Studies of eye growth in chicks have addressed whether the retina can decode the sign of defocus as this may play a role for emmetropization and possibly also accommodation. However, findings have not been unambiguous and questions remain. Here, we report on monocular accommodation studies of emmetropic and myopic human subjects to clarify whether foveal vision drives accommodation in the correct direction by removing out-of-focus blur potentially before relying on other cues. Subjects viewed monocularly a green target at 1-meter distance while being presented with a random sequence of negative defocus step changes induced by a pupil-conjugated current-driven tuneable lens. The natural pupil was constricted by a pupil-conjugated motorized iris using three different diameters and target brightness was set with a liquid crystal variable attenuator. A Hartmann-Shack wavefront sensor with an infrared beacon captured real-time changes of defocus and Zernike polynomial coefficients up to 4th radial order. We find that the young adult eye accommodates reliably in the correct direction but with a latency of 300 – 700 ms. The findings are discussed in relation to an absorption model of light in outer segments

that breaks the defocus symmetry and thus may serve as a plausible guide for accommodation and emmetropization.

1. Introduction

Accommodation refers to an increase in optical power of the crystalline lens required to keep retinal images in focus when viewing near objects [1]. The range of accommodation decreases with age until the onset of presbyopia at an age of approximately 40 years and beyond [2]. If the imaging light is focussed in front of the retina, the eye is overpowered resulting in positive defocus or myopic blur. In turn, if the light is focussed behind the retina, the eye is underpowered resulting in negative defocus or hyperopic blur. The blur of the monochromatic 2-D point-spread-function (PSF) is symmetric with respect to positive and negative defocus alone, but in combination with other aberration terms the symmetry with respect to defocus can be broken. This happens if astigmatism [3], or any other even-order aberration, is present. In turn, odd-order aberrations have no impact on the symmetry of the PSF in the presence of defocus but do reveal PSF changes if their sign changes. Combinations of even and odd-order aberrations result in shape changes of the PSF in response to defocus. The effects of even and odd-order aberrations as possible cues to accommodation have been reported by others [4,5]. The human eye has typically positive spherical aberration when relaxed but decreasing spherical aberration when accommodated with a corresponding change in the PSF [6,7]. Yet, correction with adaptive optics (AO) shows that monochromatic aberrations are not essential guiding factors for accommodation [8]. Chromatic aberrations [9-11] and the Stiles-Crawford effect of the first kind (SCE-I) [9,12,13] have both been suggested to provide cues for accommodation, as has monocular vergence [9,14,15]. Since the photoreceptors of the retina are elongated cells with a high aspect ratio it appears plausible that vergence will impact the three-dimensional PSF of the eye, and thereby the visual response via the fraction of absorbed light along the outer segments, showing that a more detailed understanding of the light-retina interaction is needed [16]. The three-dimensional structure of the retina may break symmetry to defocus in the fraction of light overlapping with the visual pigments [17] and thereby serve as a potential optical signal that is sensitive to defocus values even below ±0.125 dioptres [4,16].

Studies with animals have been done to gain insight into the relationships between defocus, eye growth and emmetropization [18]. Chicks fitted with negative power lens goggles show an increased rate of eye growth via a closed-loop mechanism that keep retinal images in focus while the eye becomes increasingly elongated and myopic [19]. Relatedly, wearing translucent occluders causes open-loop vitreous chamber growth in search of improved image quality [20,21]. Even with sectioning of the optic nerve, initial eye growth is in the correct direction

that compensates defocus, although the eye eventually overshoots emmetropization possibly due to a lack of neural feedback [22,23]. In other studies, cyclopleged chicks were placed at the centre of a drum so that only one viewing distance was possible. Yet, even with different defocus lenses, eye growth was always in the correct direction of emmetropization [24]. These findings suggest that the retina itself can detect the sign of defocus [25]. Thus, the same or related optical mechanisms may be at play in accommodation and emmetropization of the eye.

Different methods have been used to deduce characteristics of accommodation. Small fluctuations (<0.3 dioptres) have been found and suggested to play a possible role for accommodation [9,26]. With the use of an infrared optometer temporal characteristics of accommodation to step changes have been analysed alternating mechanically between two or more viewing distances [27-29] and age-dependent reaction times have been reported in the range of 0.17 s – 0.57 s [30]. Alternatively, accommodation has been studied with sinusoidal variations at different speeds finding a delay in accommodation with the largest concomitant response at approximately 4 Hz and increased fluctuations at low speeds using mechanical motion [31], or with a Badal system in combination with AO wavefront correction ruling out that monochromatic aberrations are required for accommodation [9]. Finally, ray-based wavefront sensors [32] and Hartmann-Shack wavefront sensors (HS-WFS) [33-35] have been used to capture additional wavefront information during the accommodative process for both low and high-order aberrations.

In this study, we report on temporal dynamics of monocular accommodation for both emmetropic and myopic subjects viewing through a current-driven tuneable lens (TL) that has been coded to generate a random sequence of step defocus changes within the accommodative range of each subject. TL'es are increasingly being used for defocus control and manipulation in visual optics [36,37] but to our knowledge this is the first time that a TL is directly used to trigger an accommodative response. With the random sequence, subjects receive no cue on the induced defocus. This differs from other accommodation studies using step changes or a sinusoidal variation between near and far vision whereby subjects may be able to predict the required response. Accommodative changes and aberrations were tracked at approximately 20 Hz with a HS-WFS using an infrared beacon. Subjects viewed through their natural pupil, although a motorized iris was used to set the effective pupil diameter smaller than the eye pupil both in the viewing and wavefront sensing paths and thereby exclude a possible effect of pupil miosis.

2. Material and Methods

A monocular vision system has been designed as shown schematically in Fig. 1. It uses of a current-driven TL (Optotune™ EL-16-40-TC-VIS-5D-C) which can induce defocus changes within a current range of ± 250 mA. This corresponds to a range of -3.34 to +4.56 dioptres when calibrated with the HS-WFS. The TL was evaluated with the HS-WFS in a single-pass setup separately from the accommodative studies, and it was confirmed that in all cases defocus changes were dominant as other Zernike coefficients (predominantly coma and astigmatism) accounted for less than 0.2% of the total change. The nominal response and settling times of the TL are 5 ms and 25 ms, respectively.

Subjects viewed with their right eye a green Maltese cross target on an otherwise dark computer monitor covering a 0.86° visual angle. The spectrum of the monitor peaks at 540 nm with a 70 nm bandwidth (full-width-half-maximum) as measured with an Ocean Optics™ USB2000 spectrometer and thus it is slightly narrower than the absorption spectrum of M cones. Subjects were not dilated but the room was dark to ensure a sufficiently large pupil. The left eye was occluded with a patch. The monitor was placed at 1-meter distance in front of the TL and negative defocus changes with respect to a 1-dioptre accommodative bias setting were tested. A motorized iris diaphragm (Standa™ 8MID18-1-AR) was used to limit the effective pupil diameter to 2.5, 3.5 or 4.5 mm respectively. A liquid crystal variable attenuator (Meadowlark™ LVA-100-λ) was used to adjust the image brightness. A slightly offset near-IR laser beacon (Edmund Optics™, wavelength 850 nm) was used for sensing of the ocular aberrations with a CMOS-based HS-WFS (Thorlabs™ WFS20-5C) operating at 20 Hz and capturing wavefronts up to the 4th radial Zernike order while tracking the pupil. The TL, the iris, and the HS-WFS were all mounted in conjugated pupil planes and the entire system computer controlled via a Labview (National Instruments™) programme. The calibration of the system was done prior to data collection using a mirror in the pupil plane. To limit unwanted head motion, subjects used a bitebar. Before the measurements, subjects were asked to adjust the TL focus to determine their subjective and age-dependent preferred accommodative range beyond the 1-dioptre accommodation for the visual target. The accommodation in dioptres was derived from the Zernike defocus coefficient C_{20} scaled to the appropriate pupil size.

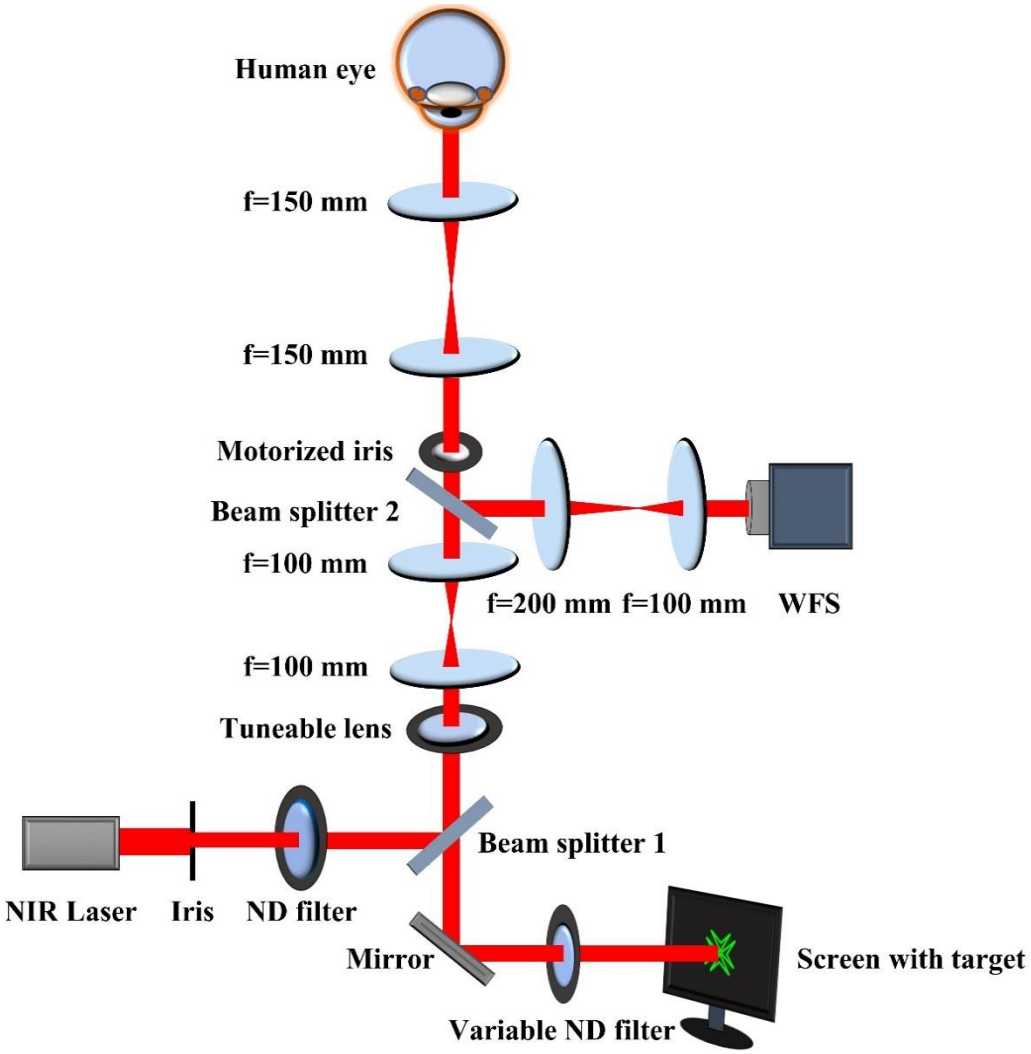

Figure 1: Schematic of the monocular vision system used to measure foveal accommodative response as a function of defocus. Three 4-*f* telescopic systems were used to map the motorized iris, HS-WFS, and TL onto the pupil plane of the eye. Beam splitter 1 is a hot mirror whereas beam splitter 2 is a 50/50 coated plate. A variable attenuator neutral density (ND) filter was used to adjust target brightness.

2.1 Participants

Ten participants took part in the study: 5 emmetropic and 5 myopic subjects with mean age 35±7.5 years and 25±2.3 years, respectively. All had healthy eyes and myopic subjects wore their spectacle glasses during measurements. The study has been approved by the UCD Human Research Ethics Committee – Sciences. Subjects read and signed an informed consent form before participation, and the study was performed in accordance with the declaration of Helsinki involving human subjects. Table 1 summarizes the age and refractive error of the right eye for all subjects. The refractive error was determined with the EyeNetra^{TM} autorefractor (with a nominal error of 0.35 dioptres). The accommodative range was determined in the

system by letting subjects adjust the TL from zero to its maximum negative power prior to the measurements while accommodating to the visual target.

Table 1: Subject and refractive error in dioptres (D) of their right eye. The comfortable accommodative (Ac) range was determined with the TL by each subject. Subjects #6 - #10 wear glasses whereas subjects #1 - #5 are uncorrected and classify as emmetropes. The subjects already accommodate 1 dioptre (bias setting) due to the 1.00 m target viewing distance.

Subject	#1	#2	#3	#4	#5	#6	#7	#8	#9	#10
Age (Years)	29	28	34	36	49	29	25	24	22	24
Sphere (Dpt)	-0.50	-0.75	-0.75	-0.75	-0.25	-0.75	-1.50	-3.00	-5.50	-6.00
Cylinder (Dpt)	0.00	0.00	0.00	0.00	0.00	-1.25 Angle 7°	-1.00 Angle 180°	-0.50 Angle 5°	-0.50 Angle 105°	-2.25 Angle 15°
Ac. range (Dpt)	-3.40	-3.53	-2.42	-2.35	-1.70	-2.90	-2.89	-2.28	-2.56	-3.28

For the emmetropes (#1 - #5) the accommodative range was smallest for the oldest subjects whereas for the younger myopes (#6 - #10) this was not the case. This may be due to uncorrected refractive errors, spectacle reflections, or the fact that the emmetropic subjects are all more experienced subjects. The average accommodative range determined for the emmetropic subjects equals 2.68 Dpt. whereas for the myopic group it equals 2.78 Dpt.

2.2 Procedures

Before the measurements, each subject was informed about the method, and that they should look onto the visual target while trying to maintain focus. For the most trained subject (#1) a duration of 200 seconds was used, whereas for the other subjects (#2 - #10) 110 seconds were used to limit fatigue. The TL generated random rapid step focal shifts (within the range set by the subject) every 10 seconds for the duration of the data collection. The same sequence of random defocus was used for all subjects but scaled to their individual accommodative range. The randomness of the shifts was used to ensure that subjects did not learn or predict the required accommodation. The participants took short breaks (5 to 7 minutes) between measurement iterations to relax. Two sets of measurements were completed with three different

pupil sizes: 2.5 mm, 3.5 mm and 4.5 mm respectively. The first set was taken without adjusting the target brightness whereas, in the second set, the transmission of the tuneable attenuator was set inversely proportional to the area of the iris diaphragm to compensate for the increase of brightness with larger pupil diameter.

3. Experimental Results

Fig. 2 shows the temporal accommodation variation for emmetropic subject #1 using three different diaphragm diameters in response to a random sequence of TL focal changes. Pupil blinks have been supressed using Matlab™ processing without affecting other aspects of the temporal response. The largest change of the TL for this subject is equivalent to -2.4 dioptres in addition to the 1-dioptre bias accommodation of the subject. As can be seen, accommodation follows in all cases the induced focal changes of the TL closely. The measurements were first done with a constant neutral density setting of the tuneable attenuator and subsequently by reducing the transmission of the filter for large iris settings to compensate the increase in pupil area. As can be seen, the different level of brightness has no significant impact. Thus, pupil-compensated brightness was not used for all the 10 subjects.

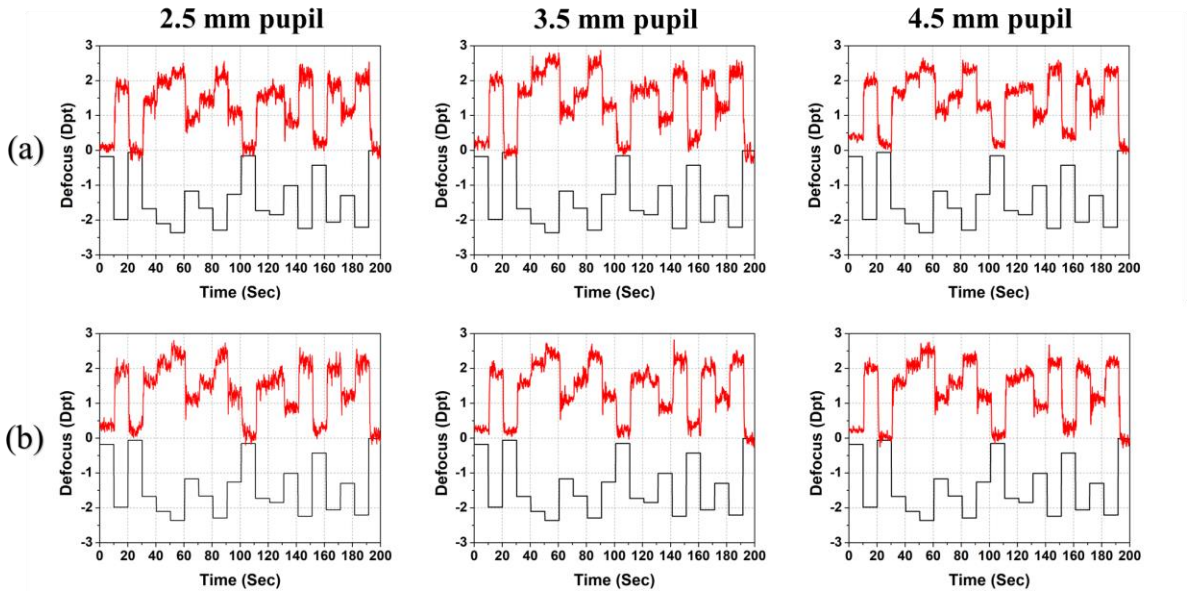

Figure 2: Defocus (TL: black line) and accommodation (eye: red line) as a function of time for an emmetropic subject (#1) with three different iris diaphragms: 2.5 mm, 3.5 mm and 4.5 mm (a) with and (b) without adjustment of the brightness to compensate pupil area.

To examine the possible role of other monochromatic aberrations simultaneously-captured Zernike coefficients are shown in Fig. 3 for defocus, astigmatism, spherical, and root-mean-square (RMS) of the measured wavefront (excluding tip and tilt) for the same case as shown in Fig. 2. As can be seen, the RMS value follows closely the Zernike coefficient for defocus. Careful comparison of the coefficients shows a slight change in 4th-order spherical aberration Z_{12} at each defocus Z_4 change, but with opposite sign, confirming the common observation of negative spherical aberration with increased accommodation [7,38]. Relatedly, there are also very small changes in astigmatism where Z_3 tends to change with the same sign as Z_4 whereas Z_5 tends to change with the opposite sign. In some cases (not shown) also minute changes in coma were noticed where Z_7 and Z_8 changed with the same sign as defocus. In all cases, however, these changes are very minor as seen in Fig. 3(b) and the scaled RMS of the wavefront follows closely that of defocus only.

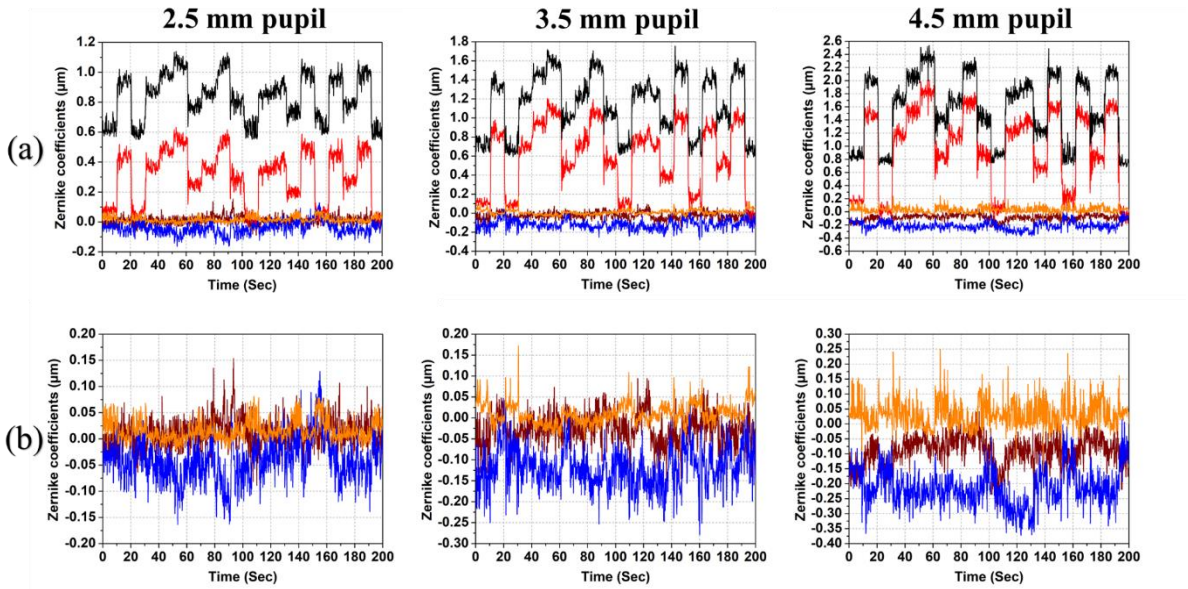

Figure 3: (a) Individual Zernike coefficients (subject #1) with three different iris diaphragms: 2.5 mm, 3.5 mm and 4.5 mm for defocus Z_4 (red line), astigmatism Z_3 and Z_5 (brown line and blue line, respectively), and spherical Z_{12} (orange line). Additionally, the total RMS of all Zernike coefficients, excluding tip and tilt, is shown (black line). Note that the RMS in (a) has been shifted vertically by 0.5 μm for ease of viewing. In (b) a magnified view is shown for the same cases including only astigmatism and spherical aberration terms.

Fig. 4 shows examples of accommodation for emmetropic subjects #2 and #3 with three different iris diaphragms. The random sequence is the same as used in Fig. 2 but scaled to the accommodative range of the subjects and interrupted at 110 seconds. As expected, the

accommodative range is smaller for subject #3 than subject #2. A small accommodative overshoot can be seen in some cases. Subject #2 underaccommodated slightly with the larger pupil sizes.

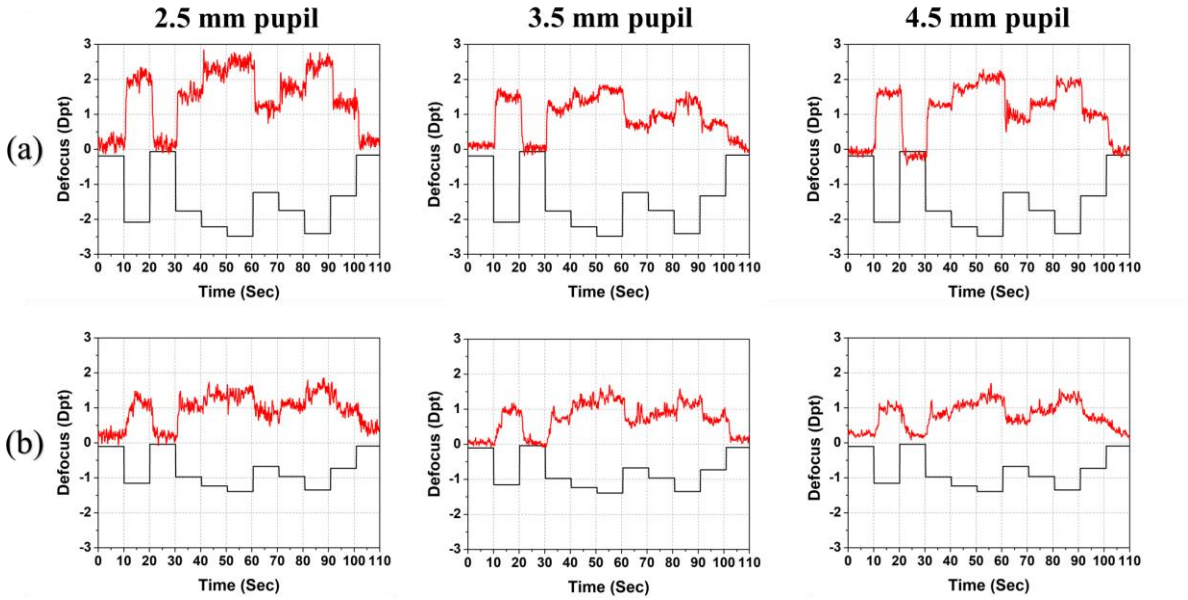

Figure 4: Defocus (TL: black line) and accommodation (eye: red line) as a function of time for two emmetropic subjects (a) #2 and (b) #3 with three different iris diaphragms: 2.5 mm, 3.5 mm and 4.5 mm and constant neutral density setting of the variable attenuator.

All myopic subjects were instructed to wear their personal spectacle corrections during measurements. Fig. 5 shows examples for two myopic subjects. Again, a very small accommodative overshoot can be seen in some cases. Also, with the larger pupil noise has increased for one subject as seen in Fig. 5(b). This may relate to fatigue or possible reflections in the spectacle lenses worn by the subject.

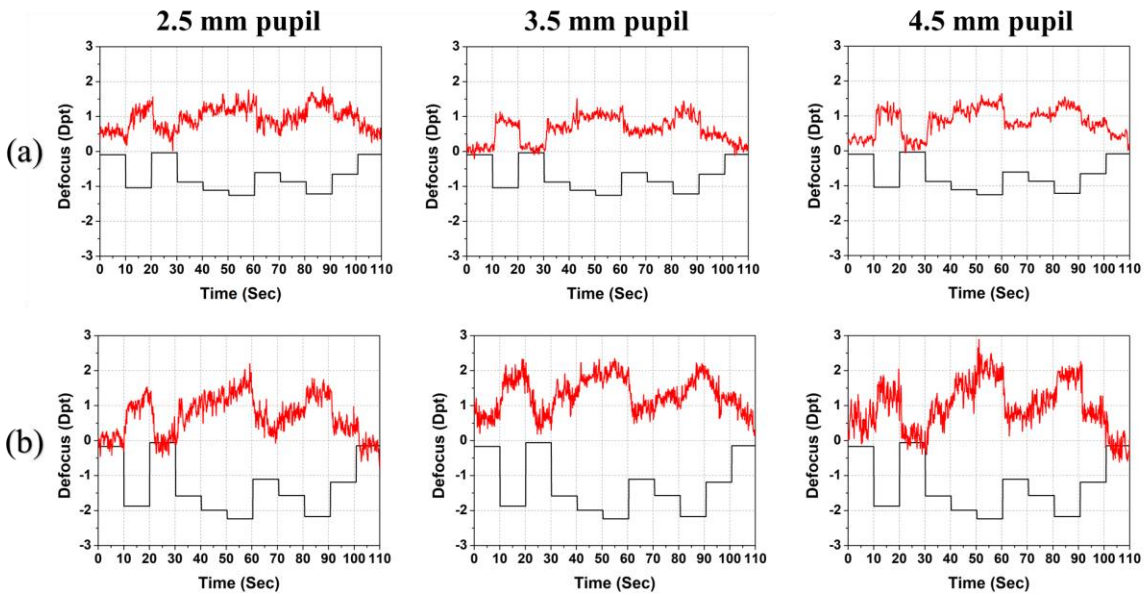

Figure 5: Defocus (TL: black line) and accommodation (eye: red line) as a function of time for two myopic subjects (a) #8 and (b) #10 with three different iris diaphragms: 2.5 mm, 3.5 mm and 4.5 mm and constant neutral density setting of the variable attenuator.

Other subjects showed similar tendencies, and a reduced range with age. Some subjects found the measurements more challenging than others. The analysis shows that all subjects accommodated in the correct direction to compensate defocus induced by the TL although in all cases small temporal fluctuations were continuously present. The temporal response of each subject varied with the magnitude of the defocus step as well as with the pupil size. For the presbyopic subject (#5) pupil miosis was also noted when accommodating. As an example, we have analysed the 11 sec – 19 sec interval in more detail for the emmetropic and myopic subjects by calculating the standard deviation of the defocus signal. The microfluctuations are largest for the younger (myopic) subjects at all pupil sizes by up to 30% when compared to the emmetropic subject group with the 4.5 mm pupil. In turn, the oldest subject (#5) has on average the smallest microfluctuations.

Fig. 6 shows examples of the temporal dynamics of accommodation for two of the subjects. For all subjects, the reaction time (latency or delay in the onset of accommodation after a TL defocus change) was in the range of 300 – 700 ms and the response time 200 – 800 ms (time required to complete accommodation before stabilizing at a new accommodative level). The response for far-to-near accommodation was faster than near-to-far relaxation for all subjects. These findings are in good agreement with time intervals reported by others [2,28]. Also, the oscillatory behaviour seen in the data is in good agreement with the accommodative

oscillations reported by others [26]. There were no marked differences between emmetropic and myopic subjects analysed in terms of the magnitude of the oscillations or temporal dynamics of the accommodation and the main differences may stem from the fact that they myopic subjects were younger and less trained subjects.

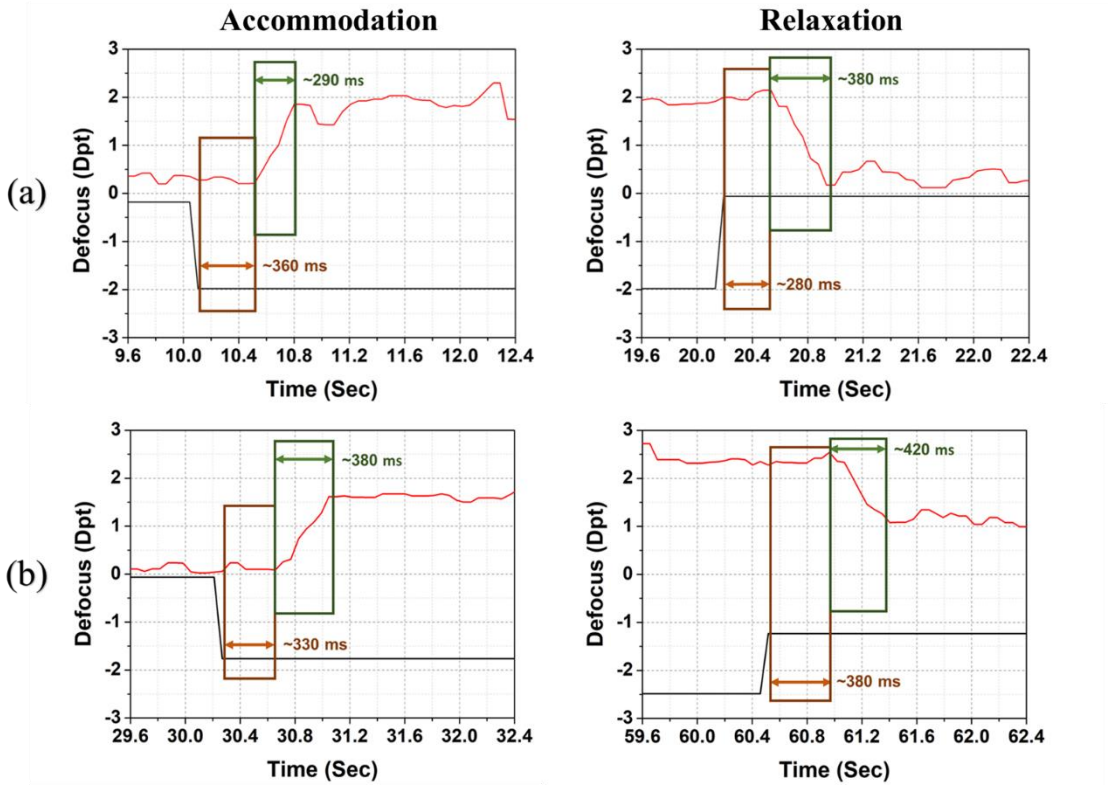

Figure 6: Examples of detailed temporal dynamics, defocus (TL: black line) and accommodation (eye: red line), of a step change for accommodation (left) and relaxation (right) for two subjects (a) #1 and (b) #2. The determined reaction (brown rectangle) and the response (green rectangle) times are indicated.

4. Physical optics model for absorption in visual pigments

The determined reaction time cannot exclude a possible conscious contribution to accommodation since early neural processing at 70 ms has been reported [39]. The often-prolonged response time is likely driven, at least partially, by a conscious decision in search of the best focus. Animal studies have shown that emmetropization is controlled locally during eye growth. Thus, it appears plausible that the developing eye can detect the sign of defocus even without neural processing [24,25]. If so, this may add an unconscious element, in the optics of the retina itself, to the defocus decision making. Photoreceptors are commonly described as biological waveguides [40,41]. However, this does not accurately account for the role of nonguided light. We have recently introduced an absorption model for the visual

pigments in the outer segments based on ray optics [17]. The model does not enforce waveguiding and thus accounts for all light traversing the neural retina by estimating the fraction of absorbed light that triggers vision. It successfully describes the integrated effect of light traversing the pupil in the Stiles-Crawford effect. Fig. 7 shows a schematic of this model for foveal vision. The same principle can be extended to the parafoveal retina when analysing peripheral accommodation and emmetropization [42]. Since cones are pointed towards a common pupil point [43] the outer segment tips are less densely packed than the cone inner segments. Thus, visual pigments are more densely packed in the anterior than in the posterior outer segments albeit the difference is small for the foveal cones. An axial pigment density gradient is more significant for the peripheral retina due to the prominent conical shape of parafoveal outer segments.

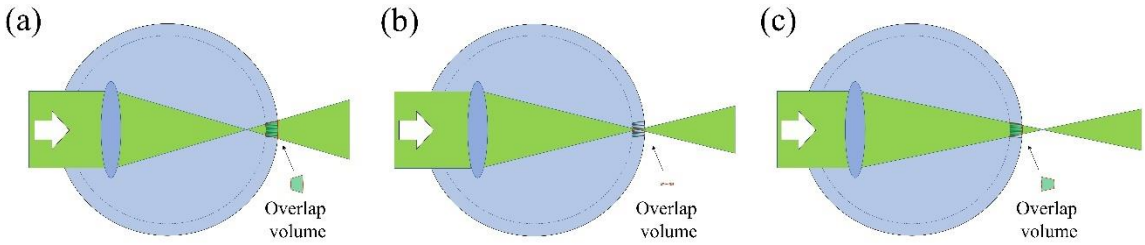

Figure 7: Schematic of foveal defocus in the volumetric absorption model for photoreceptor outer segments: when light is focussed (a) in front, (b) in the middle, (c) or beyond the retina. Small insets show the overlap volume between light and densely packed visual pigments.

The 3-D structure of the retina breaks the symmetry of defocus in the fraction of absorbed light. The volumetric absorption model [17] describes the visibility as being proportional to the volume of visual pigments exposed to light. This intersection volume can be seen schematically with the insets in Fig. 7. Due to the dense packing of foveal cones the overlap is proportional to the volume of the light spread across the outer segments. The light intensity is highest when focussed on the photoreceptors, whereas if the light is focussed in front or behind the retina the intensity is less across the outer segments. The in-focus concentration of light from a distant point source provides the highest signal and contrast at focus (Fig. 7). In turn, if viewing an extended complex object, light will spread across a larger retinal area with adjacent cone cells, but contrast will still be highest when the object is in focus. This will be the case when monocular vergence of light is matched to remain confined within each outer segment. The geometrical modelling concept can be extended to electromagnetic models for the retina as we have done when analysing the Stiles-Crawford effect [16]. Fig. 8 shows calculations with

defocus for a schematic eye with axial length f_{eye} = 22.2 mm, outer segment length of 50 μm, and centre-to-centre cone spacing of 2.5 μm. It should be stressed that Fig. 7 and Fig. 8 exclude aberrations. This is a fair approximation for the small eye pupil, but it could have an impact for larger pupils by deviating light rays, increasing light leakage, and reducing visual contrast.

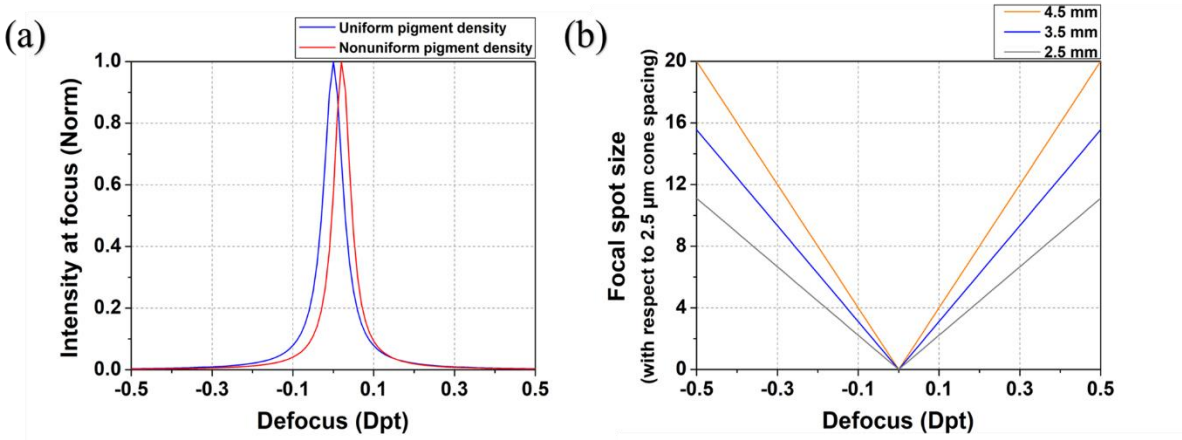

Figure 8: Calculated role of defocus with the volumetric absorption model for photoreceptor outer segments where positive defocus implies focussed in front of the retina and negative defocus behind. In (a) the role of defocus is shown for the volume of light when normalized to the volume at best focus as shown in Fig. 7(b). The uniform pigment density plot is for a uniform distribution of pigments along the outer segment length, whereas the nonuniform pigment density plot is for a gradual drop of pigment density to 50% along the outer segment length (as would be the case with slightly conical outer segments). In (b) the average focal spot size (diameter) is shown with defocus and when normalized to a 2.5 μm cone centre-to-centre cone spacing for three pupil diameters: 2.5, 3.5 and 4.5 mm. The highest contrast is when imaging light is confined to individual outer segments as achieved with a small pupil and negligible defocus blur.

Fig 8(a) corresponds to the case of looking onto a point object and with the highest concentration of light at focus. The distribution is symmetric with respect to 0 dioptres when the density of pigments is uniform, but a nonuniform pigment density shifts the symmetry which for emmetropization implies a slight translation to best focus in front of the retina. The newest pigments are located near the cone ellipsoid whereas older pigments are located near the outer segment tips. Thus, it seems plausible that there is an absorption gradient along the axis of the photoreceptors. A stronger axial drop-off in pigment (such as for peripherical cones) results in a larger shift. Fig. 8(b) shows the geometry-determined averaged focal spot size when normalized to a 2.5 μm cone centre-to-centre spacing. This shows directly the effect of monocular vergence. For small pupil sizes the light is concentrated on just one outer segment

when defocus is small (< ±0.05 dioptre). With larger pupil sizes, or with more defocus, leakage from the outer segments increases and as a result visual contrast drop. Nonuniform absorption with axial length shifts slightly the curves towards positive defocus as in Fig. 8(a).

5. Discussion

We found no evidence of fast accommodative response that could exclude neural processing. Also, no significant differences were found in reaction or response time between emmetropes and myopes which agrees well with previous studies [44]. Indeed, if subjects were tired the reaction and response times both increased (by up to 3-times) suggesting a predominantly neural drive for accommodation. Wavefront analysis showed that Zernike defocus changes were dominant for pupil sizes up to 4.5 mm and thus the role of higher-order aberrations had little if any impact on accommodation in agreement with other findings [6]. This can also be appreciated in Fig. 3 where the RMS and defocus terms are highly similar. This could be further explored with closed-loop adaptive optics vision simulators that allow accurate real-time control of both low- and high-order aberrations. Matching brightness for different pupil sizes had no measurable impact on accommodation.

From the volumetric absorption model [17] it is tempting to conclude that the eye adjusts to maximum brightness within the retina exposed to light as shown in Fig. 8(a). However, for most visual tasks, the eye views extended scenes and thus optimization of contrast is a more likely candidate to drive both accommodation and emmetropization as shown in Fig. 8(b). When the eye pupil is small, light will largely propagate within each outer segment with a minimum of leakage. Thus, contrast will be highest. For increased pupil sizes leakage becomes more prominent and contrast drops. Aberrations will further impact the effective retinal images due to the obliqueness of the light at the retina [45]. Small accommodation fluctuations have been observed in the gathered data (Fig. 2 – Fig. 6) and are in fair agreement with previously reported results [26]. These fluctuations may potentially serve to perturb contrast by changing monocular vergence and thereby outer segment light leakage to drive accommodation in the correct direction to compensate defocus.

For emmetropization of the eye, the axial gradient in visual pigments, which is largest in the parafoveal cone outer segments, seems a likely closed-loop mechanism for eye growth. Indeed, the outer segment length and density in the eye of young children at 45 months of age is approximately only 50% of the adult eye [46]. In turn, in the adult population differences in outer segment length are not large [47]. Studies in infant monkey eyes have shown that eye

growth can be altered both in a hyperopic and myopic direction when wearing lenses [48]. For animal models used for form-deprivation myopia wearing diffuser goggles [21,49], or with lid fusion [50], light will arrive onto the retina at increased oblique angles when compared to imaging light preventing it from being directionally confined within single or few outer segments. Contrast will be poorly defined and as a result eyes elongate in search of improvement and lower monocular vergence.

6. Conclusions

This study has addressed monocular accommodation with a more automated optical setup with a TL lens compared than other studies and shows that higher order aberrations has not so significant impact on accommodation and discussed it in relation to emmetropization of the human eye. The findings show that accommodation is not fast enough to exclude a conscious-driven neural accommodation response. Yet, it shows that the young eye always accommodates, or relaxes, in the correct direction to compensate defocus. It must be stressed that in normal binocular conditions additional cues for accommodation are present [51,52].

The findings have been discussed in relation to a model for monocular vergence based on a volumetric overlap of light with the visual pigments distributed throughout the outer segments. Axial differences in pigment density breaks the symmetry with respect to defocus and could be a possible candidate to drive also emmetropization. The optics model suggests that both accommodation and emmetropization operate to minimize vergence and thus light leakage along the outer segments. This 3-D modelling of the photoreceptors [16,17] open up new pathways to understand the optics of the retina in the context of vision and eye growth.

Funding

This research project is funded by the European Union's H2020 ITN network "MyFUN" under Marie Skłodowska-Curie grant agreement no. 675137.

Acknowledgement

The authors are grateful to Ms. S. Qaysi for her help with the Labview programme coding and to all subjects who kindly participated in this study.

References

1. T. Young, “On the mechanism of the eye,” Phil. Trans. Roy. Soc. 1801; **92**: 23–88.
2. W. N. Charman, “The eye in focus: accommodation and presbyopia,” Clin. Exp. Optom. 2008; **91(3)**: 207–225.
3. F. W. Campbell and G. Westheimer, “Factors influencing accommodation responses of the human eye,” J. Opt. Soc. Am. 1959; **49**: 568–571.
4. B. J. Wilson, K. E. Decker, and A. Roorda, “Monochromatic aberrations provide an odd-error cue to focus direction,” J. Opt. Soc. Am. A 2002; 19: 833–839.
5. A. I. Moulakaki, A. J. del Águila-Carrasco, J. J. Esteve-Taboada, and R. Montés-Micó, “Effect of even and odd-order aberrations on the accommodation response,” Int. J. Ophthalmol. 2017; 10: 955–960.
6. L. N. Thibos, A. Bradley, T. Liu, N. López-Gil, “Spherical aberration and the sign of defocus,” Optom. Vis. Sci. 2013; **90(11)**: 1284–1291.
7. N López-Gil, V. Fernández-Sánchez, “The change of spherical aberration during accommodation and its effect on the accommodation response,” J. Vision 2010; **10(13)**: 1–15.
8. P. Bernal-Molina, I. Marín-Franch, A. J. del Águila-Carrasco, J. J. Esteve-Taboada, N. López-Gil, P. B. Kruger, R. Móntes-Micó, “Human eyes do not need monochromatic aberrations for dynamic accommodation,” Ophthalmic Physiol. Opt. 2017; **37(5)**: 602–609.
9. E. F. Fincham, “The accommodation reflex and its stimulus,” Br. J. Ophthalmol. 1951; **35**: 381–393.
10. D. I. Flitcroft, “The interactions between chromatic aberration, defocus and stimulus chromaticity: Implications for visual physiology and colorimetry,” Vision Res. 1989; **29**: 349–360.
11. S. A. Cholewiak, G. D. Love, M. S. Banks, “Creating correct blur and its effect on accommodation,” J. Vision 2018; **18(9)**:1, 1–29.
12. P. B. Kruger, N. López-Gil, L. R. Stark, “Accommodation and the Stiles-Crawford effect: theory and a case study,” Ophthalmol. Physiol. Opt. 2001; **21**: 339–351.
13. B. Vohnsen, “The retina and the Stiles-Crawford effects,” Chapter 18 in Handbook of Visual Optics, Volume I, Ed. P. Artal (CRC Press Taylor & Francis 2017).
14. A. J. Del Águila-Carrasco, I. Marín-Franch, P. Bernal-Molina, J. J. Esteve-Taboada, P. B. Kruger, R. Montés-Micó, N. López-Gil, “Accommodation responds to optical

vergence and not defocus blur alone," Invest. Ophthalmol.Vis. Sci. 2017; **58(3)**:1758–1763.

15. I. Marín-Franch, A. J. Del Águila-Carrasco, P. Bernal-Molina, J. J. Esteve-Taboada, N. López-Gil, R. Montés-Micó, P. B. Kruger, "There is more to accommodation of the eye than simply minimizing retinal blur," Biomed. Opt. Express 2017; **8**: 4717–4728.
16. B. Vohnsen, "Directional sensitivity of the retina: A layered scattering model of outer-segment photoreceptor pigments," Biomed. Opt. Express 2014; **5**:1569–1587.
17. B. Vohnsen, A. Carmichael, N. Sharmin, S. Qaysi, D. Valente, "Volumetric integration model of the Stiles-Crawford effect of the first kind and its experimental verification," J. Vision 2017; **17(12)**:18, 1–11.
18. C. F. Wildsoet, "Active emmetropization - evidence for its existence and ramifications for clinical practise," Ophthal. Physiol. Opt. 1997; **17**: 279–290.
19. F. Schaeffel, A. Glasser, H. C. Howland, "Accommodation, refractive error and eye growth in chickens," Vision Res. 1988; **28**: 639–657.
20. J. Wallman, M. D. Gottlieb, V. Rajaram, L. A. Fugate-Wentzek, "Local retinal regions control local eye growth and myopia," Science 1987; **237**: 73–77.
21. I. G. Morgan, R. S. Ashby, D. L. Nickla, J. A. Guggenheim, "Form deprivation and lens-induced myopia: are they different?," Ophthalmic Physiol. Opt. 2013; **33**: 355–361.
22. D. Troilo, M. D. Gottlieb, J. Wallman, "Visual deprivation causes myopia in chicks with optic nerve section," Curr. Eye Res. 1987; **6(8)**: 993–999.
23. D. Troilo, J. Wallman, "The regulation of eye growth and refractive state: An experimental study of emmetropization," Vision Res. 1991; **31**: 1237–1250.
24. F. Schaeffel, S. Diether, "The growing eye: an autofocus system that works on very poor images," Vision Res. 1999; **39**: 1585–1589.
25. F. Schaeffel, C. Wildsoet, "Can the retina alone detect the sign of defocus?," Opthal. Phys. Opt. 2013; **33(3)**: 362–367.
26. F. W. Campbell, G. Westheimer, J. G. Robson, "Significance of fluctuations of accommodation," J. Opt. Soc. Am. 1958; **48**: 669.
27. F. W. Campbell, G. Westheimer, "Dynamics of accommodation responses of the human eye," J. Physiol. 1960; **151**: 285–295.
28. J. Tucker, W. N. Charman, "Reaction and response times for accommodation," Am. J. Optom. Physiol. Opt. 1979; **56(8)**: 490–503.

29. D. Shirachi, J. Liu, M. Lee, J. Jang, J. Wong, L. Stark, “Accommodation dynamics. I. Range nonlinearity,” Am. J. Optom. & Physiol. Opt. 1978; **55**: 631–641.
30. W. N. Charman, G. Heron, “On the linearity of accommodation dynamics,” Vision Res. 2000; **40**: 2057–2066.
31. F. W. Campbell, J. G. Robson, G. Westheimer, “Fluctuations of accommodation under steady viewing conditions,” J. Physiol. 1959; **145**: 579–594.
32. J. C. He, S. A. Burns, S. Marcos, “Monochromatic aberrations in the accommodated human eye,” Vision Res. 2000; **40**: 41–48.
33. C. A. Hazel, M.J. Cox, N. C. Strang, “Wavefront aberration and its relationship to the accommodative stimulus-response function in myopic subjects,” Optom. Vis. Sci. 2003; **80(2)**: 151–158.
34. N. López-Gil, V. Fernández-Sánchez, R. Legras, R. Montés-Micó, F. Lara, J. L. Nguyen-Khoa, “Accommodation-related changes in monochromatic aberrations of the human eye as a function of age,” Invest. Ophthalmol. Vis. Sci. 2008; **49(4)**: 1736–1743.
35. M. Kobayashi, N. Nakazawa, T. Yamaguchi, T. Otaki, Y. Hirohara, T. Mihashi, “Binocular open-view Shack–Hartmann wavefront sensor with consecutive measurements of near triad and spherical aberration,” Appl. Opt. 2008; **47**: 4619–4626.
36. B. Lochocki, B. Vohnsen, “Defocus-corrected analysis of the foveal Stiles–Crawford effect of the first kind across the visible spectrum,” J. Opt. 2013; **15**: 125301.
37. V. Akondi, L. Sawides, Y. Marrakchi, E. Gambra, S. Marcos, C. Dorronsoro, “Experimental validations of a tunable-lens-based visual demonstrator of multifocal corrections,” Biomed. Opt. Express 2018; **9**: 6302–6317.
38. D. A. Atchison, M. J. Collins, C. F. Wildsoet, J. Christensen, M. D. Waterworth, “Measurement of monochromatic ocular aberrations of human eyes as a function of accommodation by the Howland aberroscope technique,” Vision Res. 1995; **35**: 313–323.
39. F. Oppermann, U. Hassler, J. D. Jeschniak, T. Gruber T, “The rapid extraction of gist – Early neural correlates of high-level visual processing,” J. Cog. Neurosci. 2011; **24**: 521–529.
40. A. W. Snyder, C. Pask, “The Stiles–Crawford effect—explanation and consequences,” Vision Res. 1973; **13**: 1115–1137.
41. B. Vohnsen, I. Iglesias, P. Artal, “Guided light and diffraction model of human-eye photoreceptors,” J. Opt. Soc. Am. A 2005; **22**: 2318–2328.

42. L. Lundström, A. Mira-Agudelo, P. Artal, “Peripheral optical errors and their change with accommodation differ between emmetropic and myopic eyes,” J. Vision 2009; **9(6)**:17, 1–11.
43. A. M. Laties, J. M. Enoch, “An analysis of retinal receptor orientation. I. Angular relationship of neighboring photoreceptors,” Invest. Ophthalmol. 1971; **10**: 69–77.
44. M. L. Abbott, K. L. Schmid, N. C. Strang, “Differences in the accommodation stimulus response curves of adult myopes and emmetropes,” Ophthalmol. Physiol. Opt. 1998; **18**: 13–22.
45. B. Vohnsen, “Photoreceptor waveguides and effective retinal image quality,” J. Opt. Soc. Am. A 2007; **24**: 597–607.
46. C. Yuodelis, A. Hendrickson, “A qualitative and quantitative analysis of the human fovea during development,” Vision Res. 1986; **26**: 847–855.
47. G. Maden, A. Cakir, D. Icar, B. Erden, S. Selim Bolukbasi, M. Elcioglu, “The distribution of the photoreceptor outer segment length in a healthy population,” J. Ophthalmol. 2017; 4641902.
48. E. L. Smith III, L.-F. Hung, “The role of optical defocus in regulating refractive development in infant monkeys,” Vision Res. 1999; **39(8)**: 1415–1435.
49. J. Wallman, J. Winawer, “Homeostasis of eye growth and the question of myopia,” Neuron 2004, **43**: 447–468.
50. T. Wiesel, E. Raviola, “Myopia and eye enlargement after neonatal lid fusion in monkeys,” Nature 1977; **266**: 66–68.
51. S. R. Bharadwaj, T. R. Candy, “Cues for the control of ocular accommodation and vergence during postnatal human development,” J Vision 2008; **8(16)**: 14.1–16.
52. G. Heron, B. Winn, “Binocular accommodation reaction and response times for normal observes,” Ophthal. Physiol. Opt. 1989; **9**: 176–183.